PI3Kβ is selectively required for growth factor-stimulated macropinocytosis

Gilbert Salloum[1], Charles T. Jakubik[2], Zahra Erami[1], Samantha D. Heitz[1], Anne R. Bresnick[2,*] and Jonathan M. Backer[1,2,*]

ABSTRACT

Macropinocytosis is an actin-dependent but clathrin-independent endocytic process by which cells nonselectively take up large aliquots of extracellular material. Macropinocytosis is used for immune surveillance by dendritic cells, as a route of infection by viruses and protozoa, and as a nutrient uptake pathway in tumor cells. In this study, we explore the role of class I phosphoinositide 3-kinases (PI3Ks) during ligand-stimulated macropinocytosis. We find that macropinocytosis in response to receptor tyrosine kinase activation is strikingly dependent on a single class I PI3K isoform, namely PI3Kβ (containing the p110β catalytic subunit encoded by *PIK3CB*). Loss of PI3Kβ expression or activity blocks macropinocytosis at early steps, before the formation of circular dorsal ruffles, but also plays a role in later steps, downstream from Rac1 activation. PI3Kβ is also required for the elevated levels of constitutive macropinocytosis found in tumor cells that are defective for the PTEN tumor suppressor. Our data shed new light on PI3K signaling during macropinocytosis, and suggest new therapeutic uses for pharmacological inhibitors of PI3Kβ.

KEY WORDS: Phosphoinositide 3-kinase, Macropinocytosis, *PIK3CB*, Tumor cells, PTEN, PDGF, HGF, Rac, Circular dorsal ruffles

INTRODUCTION

Macropinocytosis is an actin-dependent but clathrin-independent endocytic process that mediates the nonselective internalization of extracellular contents (Bloomfield and Kay, 2016; Bohdanowicz and Grinstein, 2013; Swanson, 2008). Tumor cells use macropinosomes for nutrient uptake (Commisso et al., 2013; Kim et al., 2018; Palm et al., 2017), and dendritic cells use macropinosomes for immune surveillance (Canton, 2018). Viruses and protozoa hijack the macropinocytic pathway to infect target cells (de Carvalho et al., 2015; Sobhy, 2017). Macropinosomes may also serve as a platform that amplifies phosphoinositide 3-kinase (PI3K)-dependent downstream signaling (Erami et al., 2017; Yoshida et al., 2018).

Macropinocytosis occurs constitutively in immune system cells such as macrophages and dendritic cells, or in cells transformed by activated Ras or loss of PTEN (Bar-Sagi and Feramisco, 1986; Kim et al., 2018). It can also be stimulated by receptor tyrosine kinases (RTKs), G protein-coupled receptors (GPCRs) and the Wnt pathway in a variety of cell types (Ard et al., 2015; Lim and

Gleeson, 2011; Racoosin and Swanson, 1992; Redelman-Sidi et al., 2018; Roach et al., 2008). Macropinosomes are formed when circular dorsal ruffles (CDRs) form on the dorsal surface of cells, circularize into cups, and eventually seal and pinch off to form macropinosomes (Bloomfield and Kay, 2016; Bohdanowicz and Grinstein, 2013; Swanson, 2008). While there are differences in signaling mechanisms that regulate constitutive versus ligand-induced macropinocytosis (Canton et al., 2016), signaling events common to both forms include the activation of Rac1 and its downstream effector Pak1 (Dharmawardhane et al., 2000), the activation of protein kinase C (PKC) via the activation of phospholipase C (PLC), the production of diacylglycerol (Amyere et al., 2000; Swanson, 1989), and the activation of class I PI3Ks (Araki et al., 2007, 1996).

Class I PI3Ks are the sole source of phosphatidylinositol-(3,4,5)-P_3 (PIP$_3$) in cells, as well as a major source of phosphatidylinositol-(3,4)-P_2 [PI(3,4)P$_2$] via the additional action of 5′-phosphatases such as SHIP2, synaptojanin and INPP5K (Goulden et al., 2018; Hawkins and Stephens, 2016). Activation of PI3Ks during induction of macropinocytosis occurs downstream of activated RTKs, Src or Ras, but upstream of PLC/PKC (Amyere et al., 2000; Palm et al., 2017). In *Dictyostelium*, patches of PIP$_3$ form prior to the organization of the macropinocytic cup, placing PI3K activation at an early stage in the process (Veltman et al., 2016). Similarly, PI3K activation leads to the activation of Rac1 and Pak1, whose constitutive activation in mammalian cells is sufficient to activate macropinocytosis (Dharmawardhane et al., 2000; Hodakoski et al., 2019; Redka et al., 2018), presumably via stimulation of actin-dependent ruffling. However, PI3Ks are also involved in the later steps of macropinosome formation, as the sequential production of PIP$_3$ and PI(3,4)P$_2$ in macropinocytotic cups is required for sealing and scission (Maekawa et al., 2014; Welliver and Swanson, 2012; Yoshida et al., 2009).

The specific isoforms responsible for PIP$_3$ production during macropinocytosis in mammalian cells have not been previously identified. Macrophages, which express all four class I PI3K isoforms [PI3Kα, PI3Kβ, PI3Kγ and PI3Kδ; note, these are defined by the presence of the catalytic subunit p110α, p110β, p110γ or p110δ, respectively (encoded by *PIK3CA*, *PIK3CB*, *PIK3CG* or *PIK3CD*, respectively)] exhibit partial inhibition of CXCL12-stimulated macropinocytosis following treatment with selective inhibitors for each isoform, and substantial inhibition with combinations of inhibitors for PI3Kγ together with PI3Kδ, and PI3Kα together with PI3Kβ (Pacitto et al., 2017). Isoform specificity has been demonstrated in *Dicytostelium* (Hoeller et al., 2013), but class I PI3Ks in this organism do not contain a regulatory subunit, and it is difficult to directly compare them to the mammalian class I enzymes.

In this study, we used both genetic and pharmacological methods to define the PI3Ks involved in growth factor-stimulated macropinocytosis in fibroblasts and breast cancer cells. We find a

[1]Department of Molecular Pharmacology, Albert Einstein College of Medicine, Bronx, NY 10461, USA. [2]Department of Biochemistry, Albert Einstein College of Medicine, Bronx, NY 10461, USA.

*Authors for correspondence (anne.bresnick@einstein.yu.edu; jonathan.backer@einstein.yu.edu)

J.M.B., 0000-0002-0360-5692

striking requirement for PI3Kβ, and little requirement for the other isoforms. Loss of PI3Kβ expression or activity blocks macropinocytosis at an early step, before the formation of circular dorsal ruffles. PI3Kβ is also required for macropinocytosis stimulated by constitutively active Rac, suggesting additional roles for this isoform during macropinosome sealing. Finally, PI3Kβ is required for the elevated basal macropinocytosis seen in tumor cells defective for PTEN expression or activity. The demonstration of a highly selective requirement for PI3Kβ during macropinocytosis suggests that it could be a useful target in suppressing pathological processes that rely on this process.

RESULTS
Knockout of *PIK3CB* does not affect clathrin-mediated or fluid-phase endocytosis
To explore the isoform specificity of PI3K signaling during clathrin-mediated endocytosis, we generated stable NIH3T3 cells in which endogenous *PIK3CA* or *PIK3CB* were knocked out using CRISPR/Cas9; loss of the p110α or p110β subunits was confirmed by immunoblotting (Fig. 1A).

We measured internalization of [125I]-PDGF in the NIH3T3 cell lines. p110β has been previously reported to play a kinase-independent role in receptor-mediated endocytosis of the epidermal growth factor (EGF) (Ciraolo et al., 2008) and transferrin (Jia et al., 2008) receptors in mouse embryonic fibroblasts (MEFs). Surprisingly, we did not observe any significant differences in PDGF endocytosis between control and either *PIK3CA* KO or *PIK3CB* KO cells (Fig. 1B). Additionally, we measured the internalization of Lucifer Yellow, a hydrophilic marker for fluid-phase pinocytosis. Genetic ablation of p110α or p110β had no effect on the basal uptake of Lucifer Yellow (Fig. 1C).

Knockout or inhibition of *PIK3CB*/PI3Kβ but not *PIK3CA*/PI3Kα blocks growth factor-stimulated macropinocytosis
To investigate the role of PI3Kα and PI3Kβ in macropinocytosis, we incubated *PIK3CA* and *PIK3CB* KO NIH3T3 cells with tetramethylrhodamine (TMR)-conjugated 70 kDa dextran, an established marker of macropinocytosis. Consistent with previous observations (Yoshida et al., 2015), PDGF-BB-stimulated macropinocytosis in control cells led to an increase in the number of fluorescently labeled dextran-positive structures (ranging from 0.75 to 5 μm in diameter). TMR–dextran uptake peaked by 30 min (Fig. S1A). Genetic ablation of *PIK3CB* but not *PIK3CA* reduced

macropinocytosis to levels observed in unstimulated cells (Fig. 2A–C); this data was verified in a second clone for each knockout (Fig. S1B,C). We saw a similar requirement for PI3Kβ using isoform-selective kinase inhibitors. Pretreatment with the PI3Kβ-selective inhibitor TGX221 for 30 min blocked PDGF-BB-stimulated macropinocytosis to basal levels, whereas we saw no inhibition with the PI3Kα-selective inhibitors BYL719 or A66 (Fig. 2D). We also tested the role of the two other class I PI3Ks, PI3Kγ and PI3Kδ, which are expressed at low levels in NIH3T3 cells (Guillermet-Guibert et al., 2008). Pretreatment with CZC24832 or IC-87114 to selectively inhibit PI3Kγ or PI3Kδ, respectively, had no effect on PDGF-BB-stimulated macropinocytosis (Fig. 2E). Taken together, these data suggest that PI3Kβ is the sole class I PI3K regulating PDGF-BB-stimulated macropinocytosis in fibroblasts.

To determine whether the isoform-specific contribution of PI3Kβ to macropinocytosis is unique to fibroblasts, we measured macropinocytosis in MDA-MB-231 breast cancer cells. Hepatocyte growth factor (HGF) has been previously reported to induce membrane ruffling and actin reorganization in MDCK and KB cells (Nishiyama et al., 1994; Ridley et al., 1995). Stimulation of quiescent MDA-MB-231 cells with HGF induced a robust macropinocytic response, and selective inhibition of PI3Kβ, but not PI3Kα, PI3Kγ or PI3Kδ abolished HGF-stimulated macropinocytosis (Fig. 2F). Taken together, these data suggest an essential and unique role for PI3Kβ in growth factor-induced macropinocytosis.

Knockout or inhibition of *PIK3CB*/PI3Kβ but not *PIK3CA*/PI3Kα blocks growth factor-stimulated circular dorsal ruffle formation
To define the mechanism by which PI3Kβ regulates macropinocytosis, we measured circular dorsal ruffles (CDRs), actin-rich structures that form at the dorsal surface of the cell and are precursors of macropinocytic cups. PDGF is known to induce circular dorsal membrane ruffling in fibroblasts (Mellström et al., 1988). *PIK3CA* or *PIK3CB* KO NIH3T3 cells were stimulated with PDGF-BB for 5 min, and CDRs were identified as actin- and cortactin-positive circular rings at the dorsal surface of cells. PDGF stimulation greatly enhanced CDR formation in control NIH3T3 cells (Fig. 3A). Importantly, genetic ablation of *PIK3CB* but not *PIK3CA* abolished PDGF-BB-stimulated CDR formation; loss of p110β expression significantly decreased both the percentage of cells forming CDRs and the area of CDRs that did form (Fig. 3A,B;
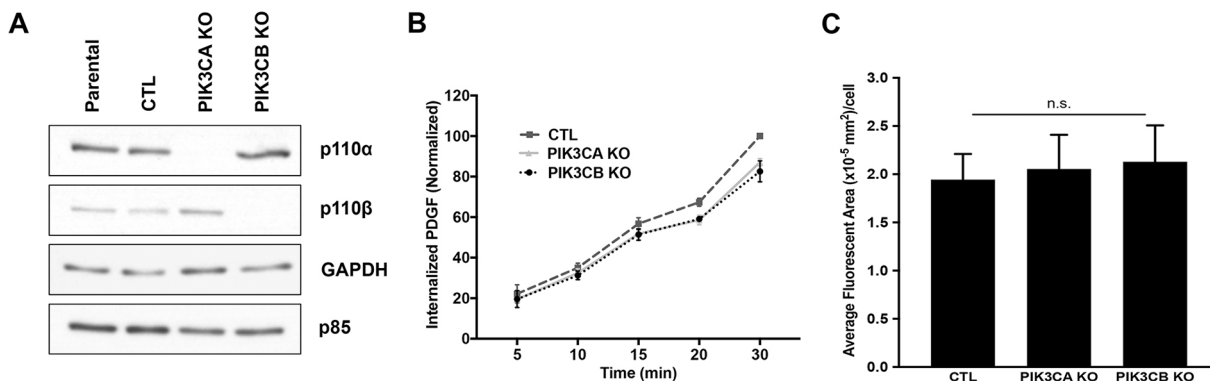

Fig. 1. *PIK3CA* or *PIK3CB* knockout does not affect clathrin-mediated or fluid-phase endocytosis. (A) Immunoblots showing expression of p110α, p110β and p85α in parental, lentiviral control (CTL) and knockout (KO) NIH3T3 lines. GAPDH was used as a loading control. (B) Internalization of [125I]-PDGF-BB by control and knockout NIH3T3 lines. (C) Lucifer Yellow uptake by control and knockout NIH3T3 lines. Data represent the mean±s.e.m. from three independent experiments (*n*≥250 cells per condition). n.s., not significant.
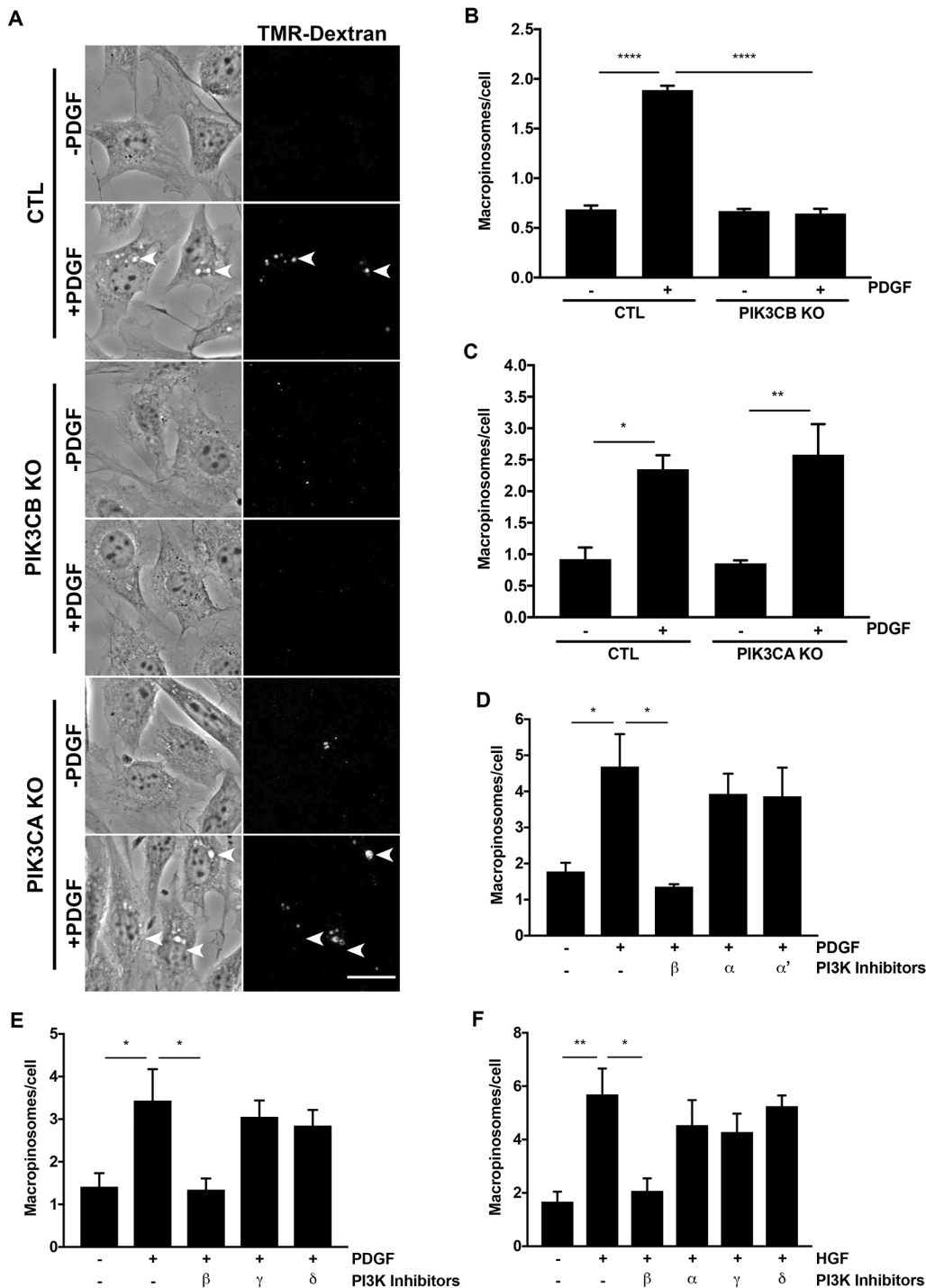
Fig. 2. Knockout or inhibition of *PIK3CB*/PI3Kβ blocks ligand-stimulated macropinocytosis in fibroblasts and breast cancer cells. (A) Representative images of PDGF-stimulated 70 kDa TMR–dextran uptake by lentiviral control NIH3T3 cells or *PIK3CB*- and *PIK3CA*-knockout (KO) cells. Scale bar: 25 µm. Arrowheads indicate positions of macropinosomes. (B) Quantification of PDGF-stimulated macropinocytosis by control and *PIK3CB*-knockout cells ($n \geq 540$ cells per condition). Macropinosomes were defined as intracellular vesicles ≥ 0.7 µm in diameter. (C) Quantification of PDGF-stimulated macropinocytosis by control and *PIK3CA*-knockout cells ($n \geq 525$ cells per condition). (D) PDGF-stimulated macropinocytosis by parental NIH3T3 cells pretreated with 0.1% DMSO, PI3Kβ inhibitor (500 nM TGX221) or two different PI3Kα inhibitors (α, 1 µM BYL719; α′, 3 µM A66) ($n \geq 610$ cells per condition). (E) PDGF-stimulated macropinocytosis by parental NIH3T3 cells pretreated with a PI3Kβ inhibitor (500 nM TGX-221), PI3Kδ inhibitor (1 µM IC-87114) or PI3Kγ inhibitor (2 µM CZC24832) ($n \geq 470$ cells per condition). (F) HGF-stimulated macropinocytosis by MDA-MB-231 breast cancer cells pretreated with isoform-selective PI3K inhibitors ($n \geq 485$ cells per condition). Data represent the mean±s.e.m. from three independent experiments. *$P < 0.03$; **$P = 0.005$; ****$P < 0.0001$.

Movie 1–3). Similar results were observed in a second clone from each knockout cell line (Fig. S2A,B). Consistent with the genetic ablation data, pharmacological inhibition of PI3Kβ but not PI3Kα almost completely blocked CDR formation in response to PDGF (Fig. 3C,D). In cells treated with the PI3Kβ inhibitor, the few CDRs that did form had significantly smaller areas as compared to control cells (Fig. 3E). These data suggest that PI3Kβ acts at an early step of growth factor-stimulated macropinocytosis.

Studies in primary bone marrow-derived macrophages (BMMs) have shown that the pan-PI3K inhibitor wortmannin had no effect on CDRs, but blocked the closure of macropinocytic cups into macropinosomes (Araki et al., 1996). To address the observed differences in the macropinocytic defect in macrophages versus fibroblasts, parental NIH3T3 cells were treated with the PI3Kβ-selective inhibitor TGX221 and/or wortmannin and stimulated with PDGF. Similar to what was seen with TGX221, wortmannin abolished CDR formation in NIH3T3 cells (Fig. S3A,B).

Gβγ coupling to PI3Kβ is necessary for macropinocytosis

We have previously identified point mutants in p110β that selectively disrupt its binding to Gβγ proteins (Dbouk et al., 2012), and described knockdown/rescue MDA-MB-231 breast
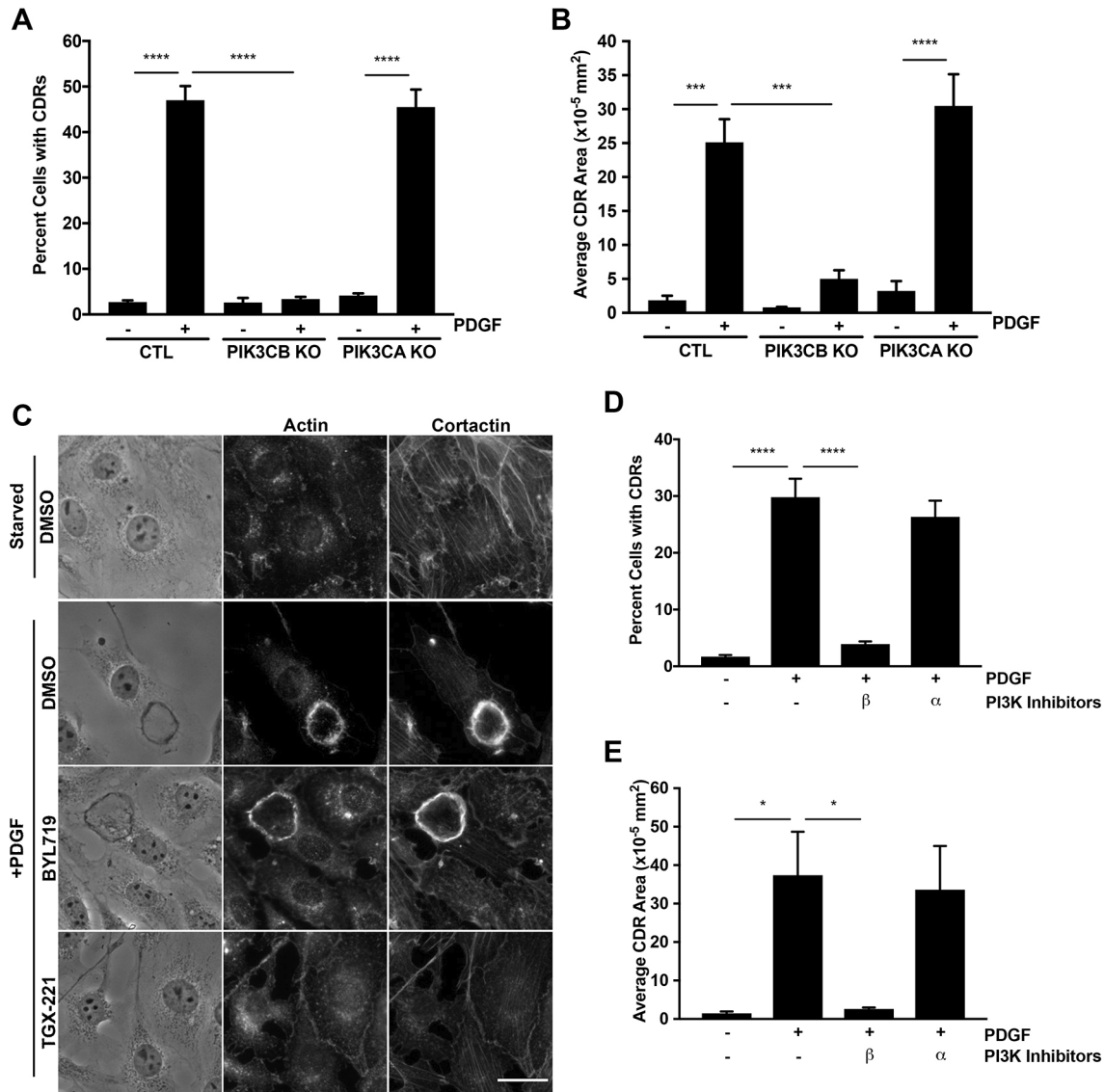
Fig. 3. Knockdown or inhibition of *PIK3CB*/PI3Kβ blocks PDGF-stimulated CDR formation in fibroblasts. (A) Starved lentiviral control or knockout NIH3T3 cells were stimulated with PDGF for 5 min. Cells were fixed and stained for actin, cortactin and DAPI, and CDRs were identified as actin- and cortactin-positive rings at the dorsal surface of cells. (B) CDR area in NIH3T3 cells was measured as described in the Materials and Methods. (C) Representative images of PDGF-stimulated parental NIH3T3 cells pretreated with isoform selective inhibitors for PI3Kα (1 µM BYL719) or PI3Kβ (500 nM TGX221). Cells were fixed and stained for actin, cortactin and DAPI. Scale bar: 25 µm. (D,E) Quantification of CDR number and area in cells treated with isoform-selective PI3Kα and PI3Kβ inhibitors. Data represent the mean±s.e.m. from three independent experiments. *P=0.04; ***P<0.0009; ****P<0.00001.

cancer cells in which endogenous human p110β was replaced with murine wild-type, kinase-dead (K-R) or Gβγ-uncoupled (KK-DD) p110β (Khalil et al., 2016). To test whether Gβγ binding to PI3Kβ is required for macropinocytosis, we used p110β-knockdown cells that were infected with lentivirus expressing wild-type or mutant HA-tagged p110β. Expression of p110β in all of the knockdown/ rescue lines was similar, although higher than in parental MDA-MB-231 cells (Fig. 4A, top). Expression of p110α was also slightly increased in the knockdown/rescue cell lines as compared to parental MDA-MB-231 cells (Fig. 4A, bottom). Control experiments showed that both lysophosphatidic acid (LPA)- and HGF-stimulated Akt phosphorylation was inhibited in cells expressing Gβγ-uncoupled p110β (Fig. 4B,C); the reduction in HGF-stimulated Akt phosphorylation was surprising, given that PI3Kα is also able to couple to activated receptor tyrosine kinases.

Macropinocytosis of 70 kDa TMR–dextran was measured after stimulation with HGF. Whereas cells expressing wild-type p110β showed levels of HGF-stimulated macropinocytosis that were similar to those seen in parental cells, cells expressing the kinase-dead or Gβγ-uncoupled p110β mutant were defective for ligand-stimulated macropinocytosis (Fig. 4D,E). These data suggest that production of free Gβγ through the activation of trimeric G-proteins is required for HGF-stimulated macropinocytosis. Consistent with these data, pretreatment with pertussis toxin (PTX) significantly blocked HGF-stimulated macropinocytosis in parental MDA-MB-231 cells (Fig. 4F).

Studies in Ras-transformed cells have suggested that PI3K activation stimulates macropinocytosis through the activation of Rac1 (Rodriguez-Viciana et al., 1997). To test this possibility, we measured dextran uptake in MDA-MB-231 cells expressing constitutively active Rac (CA-Rac), which potently stimulates
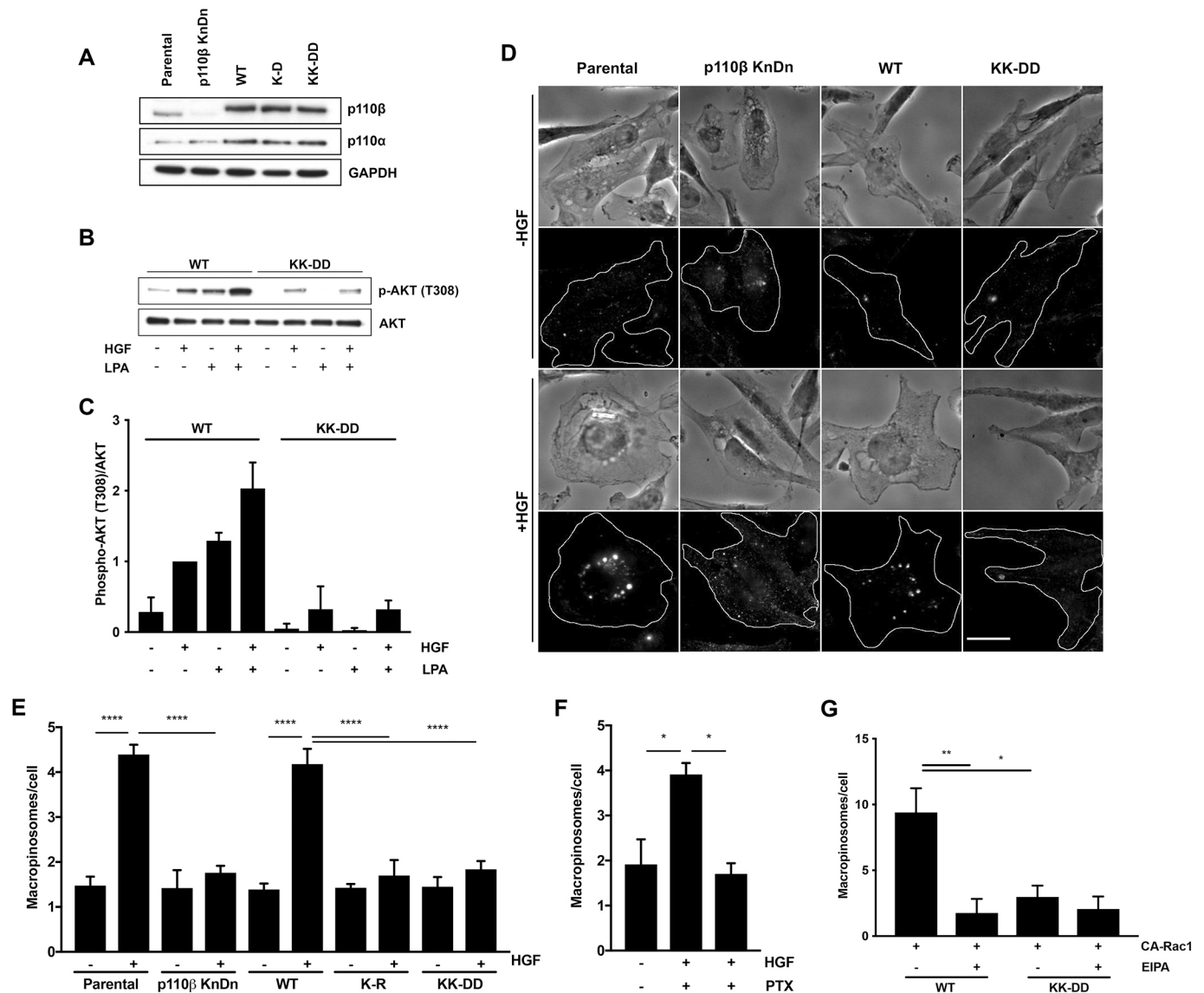
Fig. 4. Gβγ binding to PI3Kβ is required for HGF- and Rac1-stimulated macropinocytosis in breast cancer cells. (A) Western blots showing p110β and p110α expression in MDA-MB-231 p110β-knockdown cells expressing wild-type (WT), kinase-dead (K-R) or Gβγ-uncoupled (KK-DD) p110β. (B) Starved cells expressing wild-type or Gβγ-uncoupled p110β were stimulated for 5 min with 1 ng/ml HGF, 10 µM LPA or a combination of both. Cell lysates were blotted for Akt, pT308-Akt or GAPDH. (C) Quantification of pAkt:Akt ratios from immunoblots in C. (D) Representative images of PDGF-stimulated 70 kDa TMR–dextran uptake by cells expressing wild-type or mutant p110β. The cell outline is shown in white in the fluorescence images. Scale bar: 25 µm. (E) Quantification of HGF-stimulated macropinocytosis in MDA-MB-231 p110β-knockdown cells expressing WT, K-R or KK-DD p110β ($n \geq 630$ cells per condition). (F) HGF-stimulated macropinocytosis in parental MDA-MB-231 cells pretreated with pertussis toxin. (G) p110β-knockdown cells rescued with WT or KK-DD p110β were transiently transfected with GFP or CA-Rac1 (Rac1^{Q61L}-GFP). Cells were serum starved overnight and macropinocytosis was measured in the absence or presence of EIPA. Data represents the mean±s.e.m. from three independent experiments; in panel G, data represents the mean±s.d. from two independent experiments. *P=0.01; **P=0.008; ****P<0.0001.

macropinocytosis (Erami et al., 2017). Interestingly, CA-Rac-induced macropinocytosis was almost completely blocked in cells expressing Gβγ-uncoupled p110β (Fig. 4G). Thus, in addition to its role in CDR formation, PI3Kβ is required for a step in macropinocytosis that is downstream from Rac1 activation.

PI3Kβ but not PI3Kα is required for macropinocytosis in PTEN-null tumors

Previous reports have identified PI3Kβ as necessary for the growth of tumors driven by PTEN loss (Ni et al., 2012; Wee et al., 2008). Additionally, a recent study has suggested a requirement for macropinocytosis in the survival and proliferation of PTEN-null

cancers under nutrient stress. Using patient-derived xenografts and prostate cancer organoids, Edinger and colleagues described a robust constitutive macropinocytic uptake mechanism in PTEN-null tumors that is blocked by PI3K inhibition (Kim et al., 2018). We therefore examined the PI3K isoform specificity of constitutive macropinocytosis in PTEN-null tumor cells. TGX221 inhibited constitutive dextran uptake in both PTEN-deficient human breast (BT-549) (Fig. 5A,B) and prostate (PC3) (Fig. 5C,D) cancer cells, whereas inhibition of PI3Kα did not significantly affect macropinocytosis. The macropinocytosis inhibitor EIPA completely blocked TMR–dextran uptake (Fig. 5B,D). These data indicate that, in addition to growth factor-stimulated
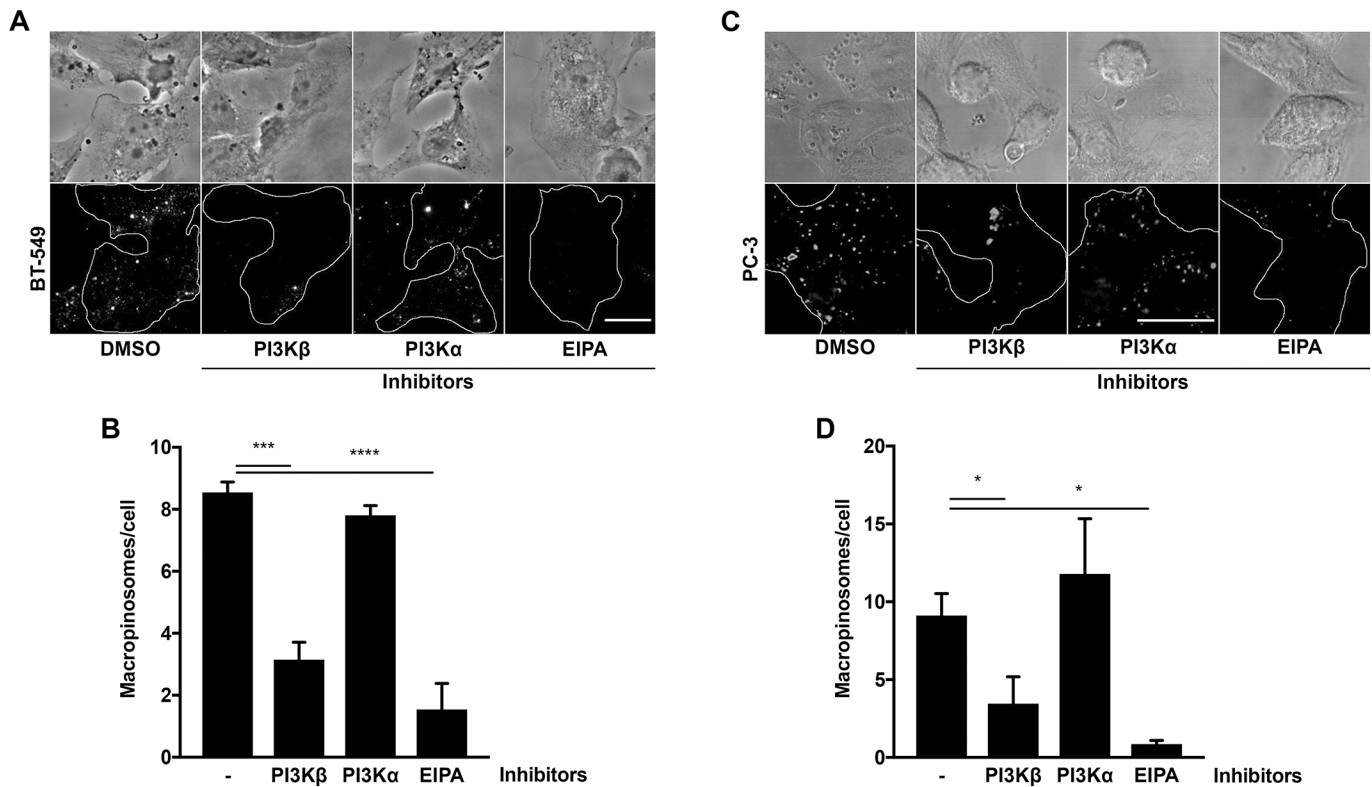
Fig. 5. Selective inhibition of PI3Kβ blocks constitutive macropinocytosis in PTEN-null cancer cells. (A) Representative images of BT-549 breast cancer cells pretreated with DMSO, TGX221, BYL719 or EIPA for 30 min, and then incubated with 70 kDa TMR–dextran. The cell outline is shown in white in the fluorescence images. Scale bar: 25 μm. (B) Quantitation of constitutive dextran uptake in BT-549 cells. (C) Representative confocal images of PC3 prostate cancer cells treated as in A. Scale bar: 30 μm. (D) Quantification of constitutive dextran uptake in PC3 cells. Data represent the mean±s.e.m. from three independent experiments. *$P<0.02$; ***$P=0.0003$; ****$P<0.0001$.

macropinocytosis, PI3Kβ has important functions in constitutive macropinocytosis in PTEN-deficient cells. This could provide a mechanism by which PI3Kβ contributes to tumor growth that is driven by the loss of PTEN.

DISCUSSION

PI3Ks are key regulators of macropinocytosis, and inhibition of this family of enzymes has been shown to block macropinocytosis in many cell types and tissues (Amyere et al., 2000; Araki et al., 1996; Kim et al., 2018). This study identifies PI3Kβ as a unique regulator of macropinocytosis in response to growth factor stimulation or loss of the tumor suppressor PTEN. By using both genetic and pharmacological inhibition of class I PI3Ks, we show that PI3Kβ is the major PI3K isoform required for growth factor-stimulated macropinocytosis in NIH3T3 cells and MDA-MB-231 breast cancer cells, and for the enhanced macropinocytosis in PTEN-null tumor cells.

PDGF stimulation of fibroblasts causes dorsal ruffling and macropinocytic cup formation, with subsequent cup closure and release of the macropinosome into the cytoplasm (Bohdanowicz and Grinstein, 2013; Mellström et al., 1988; Yoshida et al., 2015). Our data suggests that PI3Kβ is required at an early step in this process, as PDGF-stimulated CDR formation is selectively blocked by knockout or inhibition of PI3Kβ. These results are consistent with a specific requirement for PI3Kβ in apoptotic cells and Fcγ receptor-mediated phagocytosis by primary murine macrophages (Leverrier et al., 2003). However, in BMMs (Araki et al., 1996) and spleen-derived dendritic cells (West et al., 2000), the pan-PI3K inhibitor wortmannin blocked macropinocytosis but did not inhibit

early dorsal ruffle formation. Of note, while PI3Kα and PI3Kβ are ubiquitously expressed (Hiles et al., 1992; Hu et al., 1993), expression of PI3Kδ and PI3Kγ in macrophages might provide a compensatory mechanism for cells to overcome the requirement for PI3Kβ in CDR formation. In fibroblasts, which primarily express PI3Kα and PI3Kβ, we find that wortmannin does block CDR formation.

The mechanism by which PI3Kβ selectively regulates CDR formation is not known. Early studies in porcine aortic endothelial (PAE) cells have shown that PI3K inhibition blocks PDGF-stimulated membrane ruffling, and this could be rescued by the expression of wild-type or constitutively active Rac (Hawkins et al., 1995; Wennström et al., 1994). All class I PI3Ks can activate Rac1 by generating the lipid second messenger PI(3,4,5)P$_3$. Moreover, all class I PI3Ks can, in principle, be activated by GTP-bound Rac1 or Cdc42 binding to the BCR domain of the PI3K regulatory subunit p85 (Bokoch et al., 1996; Tolias et al., 1995; Zheng et al., 1994). However, PI3Kβ is the only isoform that binds to GTP-bound Rac1 and Cdc42 through its catalytic subunit (Fritsch et al., 2013); this binding is of substantially higher affinity than Rac1 binding to p85 (Heitz et al., 2019). Moreover, PI3Kβ and Rac1 can form a positive-feedback loop in PTEN-null hematopoietic stem cells (Yuzugullu et al., 2015). A positive-feedback loop between Rac1 and PI3Kβ could amplify Rac1-mediated membrane ruffling, and could be required for CDR formation.

However, we also see a complete loss of CA-Rac-stimulated macropinocytosis in MDA-MB-231 cells expressing a Gβγ-uncoupled mutant of PI3Kβ, and a partial loss in cells expressing a Rac1-uncoupled mutant (Erami et al., 2017). These data suggest

that PI3Kβ plays additional roles at later steps in the formation of macropinosomes, downstream from Rac1 activation. It is also interesting that EIPA inhibits micropinocytosis induced by CA-Rac1. It has been previously shown that EIPA inhibits micropinocytosis by reducing Rac1 and Cdc42 activation at the plasma membrane (Koivusalo et al., 2010); in cells expressing CA-Rac1, EIPA-mediated inhibition of macropinocytosis could be occurring through effects on Cdc42.

It is surprising that mutation of the Gβγ-binding site in p110β inhibited HGF-stimulated macropinocytosis and Akt phosphorylation in MDA-MB-231 cells. This suggests that optimal signaling by PI3Kβ requires dual inputs from RTKs and Gβγ, which is consistent with previous *in vitro* and *in vivo* data describing synergistic activation of PI3Kβ by RTKs and GPCRs (Dbouk et al., 2012; Houslay et al., 2016). The source of Gβγ in HGF-stimulated breast cancer cells is unknown, but could include non-receptor trimeric G-protein GEFs such as Girdin or Daple (Aznar et al., 2015; Garcia-Marcos et al., 2009; Leyme et al., 2015) or classical GPCRs responding to autocrine growth factors. For example, MDA-MB-231 breast cancer cells secrete stromal cell-derived factor 1α (SDF-1α) and express its cognate C-X-C chemokine receptor type 4 (CXCR-4) (Lee et al., 2004). Furthermore, while transactivation of GPCRs by the HGF receptor has not been described, GPCR transactivation has been documented to occur in response to activation of other RTKs (Delcourt et al., 2007). The loss of HGF signaling in cells expressing mutant p110β is not due to effects on p110α expression, which is slightly increased compared to that seen in parental cells.

Work in *Dictyostelium* cells has suggested that distinct PI3K isoforms can regulate different steps in macropinocytosis (Hoeller et al., 2013). Analysis of phosphoinositide signaling in live cells has documented the accumulation of PIP$_3$ on nascent macropinosomal membranes, after the formation of CDRs, but prior to the closure of CDRs to circular cups (Araki et al., 2007; Welliver and Swanson, 2012; Yoshida et al., 2009). PIP$_3$ then declines and PI(3,4)P$_2$ increases, presumably through the action of a 5′-phosphatase, such as SHIP2. SHIP2 has in fact been visualized in CDRS, where it is recruited by binding to the PIP$_3$-binding protein SH3YL1 (Hasegawa et al., 2011), and depletion of SHIP2 blocks macropinosome sealing in EGF-stimulated A431 cells (Maekawa et al., 2014). These data suggest a role for a class I PI3Ks in the late steps of macropinosome closure. Given that inhibition of other class I PI3Ks does not inhibit dextran uptake, we suspect that production of PIP$_3$ by PI3Kβ in the macropinocytotic cup is required for SHIP2-dependent production of PI[3,4]P$_2$. This would be consistent with our recent finding that PI3Kβ is required for the production of PI[3,4]P$_2$ in tumor cell invadopodia (Erami et al., 2019). Direct demonstration of PI3Kβ action in the cup will require experimentally bypassing its role in CDR formation; experiments to accomplish this are in progress.

Multiple reports have identified PI3Kβ as being required for oncogenic transformation and tumor growth in cancers lacking the tumor suppressor PTEN (Jia et al., 2008; Wee et al., 2008). The mechanism that links PI3Kβ to the growth of PTEN-null tumors is not yet clear. A recent study showing that macropinocytic uptake of necrotic debris serves as a nutrient uptake mechanism in PTEN-deficient tumors during times of nutrient stress (Kim et al., 2018) suggests a novel function for PI3Kβ in these tumors. Our finding that PI3Kβ is selectively required for constitutive macropinocytosis in PTEN-null cancer cells is consistent with a mechanism in which PI3Kβ-mediated macropinocytosis contributes to PI3Kβ-dependent growth and proliferation of PTEN-null tumors.

In summary, we have demonstrated a specific requirement for PI3Kβ to mediate macropinocytosis in both ligand-stimulated and in PTEN-null cells. PI3Kβ acts at an early stage in this process, promoting the formation of CDRs that mature into macropinocytotic vesicles. These data suggest that pharmacological inhibition of PI3Kβ could be therapeutically useful in disorders such as viral entry into host cells or nutrient scavenging by tumor cells that depend on robust macropinocytosis.

MATERIALS AND METHODS
Antibodies and reagents
Fibronectin from human plasma (F2006) was purchased from Sigma-Aldrich. Antibodies against phospho-Akt (Thr308) (1:1000, #13038), Akt (1:1000, #9272), p110α (1:1000, #4249), p85 (1:1000 #4257) and GAPDH (1:5000, #2118) antibodies for western blot analysis were purchased from Cell Signaling Technology. p110β antibody (1:1000, ab151549) was purchased from Abcam, or produced in-house from rabbits immunized with a KLH-coupled peptide from the C-terminal 16 amino acids of human p110β (Khalil et al., 2016). Cortactin antibody (1:200, 05-180) was purchased from Millipore Sigma. HRP-linked horse anti-mouse IgG (#7076) and goat anti-rabbit IgG (#7074) were purchased from Cell Signaling Technology. Alexa Fluor® 488–phalloidin (#8878) was purchased from Cell Signaling Technology, Alexa Fluor™ 647 goat anti-mouse IgG (H+L) (A21235) was from Invitrogen, and DAPI Fluoromount-G® (0100-20) was from SouthernBiotech. For transient transfection, Lipofectamine 3000 (L3000-015) was purchased from Life Technologies. Recombinant human PDGF-BB (220-BB) and recombinant human HGF (294-HG) were obtained from R&D Systems. Tetramethylrhodamine-conjugated dextran (TMR–dextran), 70,000 Da (D1818) was obtained from Molecular Probes. TGX221 (S1169) and CZC24832 (S7018) were purchased from Selleckchem, A66 (SML1213) and pertussis toxin (PTX) were from Calbiochem (516561). Wortmannin (W1628), EIPA (A3085) and AS1949490 (SML1022) were from Sigma-Aldrich. BYL719 and IC-87114 were gifts from Novartis and Professor Peter R. Shepherd (The University of Auckland, New Zealand), respectively.

Cell culture
Murine embryonic fibroblasts NIH3T3 (CRL-1658), human breast cancer cells MDA-MB-231 (HTB-26), human breast cancer cells BT-549 (HTB-122) and the human prostate cancer cell line PC-3 (CRL-1435) were obtained from the American Type Culture Collection (ATCC). MDA-MB-231 and NIH3T3 cell lines were maintained in Dulbecco's modified Eagle's medium (DMEM) (Gibco) supplemented with 10% fetal bovine serum (FBS) (Atlanta Biologicals) and 1% sodium pyruvate (GE Healthcare, SH30239.01). BT-549 cells were grown in Roswell Park Memorial Institute (RPMI 1640) medium (Gibco 11875-093) supplemented with 10% FBS, 1% sodium pyruvate and 0.023 IU/ml insulin. PC-3 cells were grown in Ham's F-12K (Kaighn's) Medium (21127-022) supplemented with 10% FBS and 1% sodium pyruvate. Cells were tested for mycoplasma every 6 months.

Generation of knockout and knockdown/rescue cell lines
PIK3CA-knockout (KO) NIH3T3 cells were generated using CRISPR/Cas9-targeted genome editing. Briefly, cells were infected with separate iCRISPR/Cas9 and sgRNA mouse lentiviral vectors (Applied Biological Materials; target sequence: 5′-CCGTGAGGCCACACTCGTCA-3′) and selected using Geneticin (Gibco, 11811-031) and puromycin (Sigma-Aldrich, 61-385-RA). Clonal lines were derived by limiting dilution. Knockout was confirmed by western blotting and next-generation sequencing (NGS). *PIK3CB* KO NIH3T3 cells were generated using an iCRISPR/Cas9 and sgRNA all-in-one mouse lentivial vector (Applied Biological Materials; target sequence: 5′-CCTCATGGACATTGACTCGT-3′) and selected using puromycin. Clonal lines were derived by limiting dilution. Knockout was confirmed by western blotting and Sanger sequencing.

The development of p110β-knockdown MDA-MB-231 cells using lentiviral shRNA has been previously described (Khalil et al., 2016). HA-tagged murine wild-type, kinase-dead (K799R; K-R) and Gβγ-uncoupled

(K532D-K533D; KK-DD) p110β lentiviruses were used to express p110β in the knockdown cells. Stable cell lines were selected by using blasticidin (10 µg/ml, InVivoGen). Expression of exogenous p110β was confirmed by western blotting.

Inhibitor treatments

Inhibitors were added in medium containing 0.5% FBS and 0.2% BSA for 30 min prior to the assays at the following concentrations: TGX221 (500 nM), BYL719 (1 µM), CZC24832 (2 µM), IC-87114 (1 µM), and EIPA (75 µM). PTX pretreatment (200 ng/ml) was carried out overnight before the assays. Wortmannin pretreatment (100 nM) was performed in medium in the absence of FBS or BSA.

PDGF endocytosis

Control, *PIK3CA*- or *PIK3CB*-knockout NIH3T3 cells were plated in 24-well dishes. Cells were starved overnight in DMEM containing 0.5% FBS and 0.2% BSA, and then incubated in the presence of [^{125}I]-PDGF-BB (50,000 c.p.m./ml; Perkin Elmer). After incubation for 5–30 min, cells were washed three times for 5 min each in PBS/0.1% BSA or 200 mM acetic acid with 500 mM NaCl and 0.1% BSA, to measure total cell-associated and internalized PDGF, respectively. Cells were lysed in 0.1% NaOH with 0.1% SDS and counted in a gamma counter.

Lucifer Yellow uptake assay

NIH3T3 cells were seeded in 35 mm MatTek dishes (MatTek Corporation, P35G-1.5-14-C) coated with 10 µg/cm^2 fibronectin and cultured overnight in complete medium. Lucifer Yellow was added to the cells at 1 mg/ml for 30 min at 37°C. The MatTek dishes were placed on ice, washed five times with ice-cold PBS, fixed with 4% paraformaldehyde (PFA) in PBS for 20 min at room temperature, washed three times with PBS and mounted. Images were collected using an Olympus IX70 inverted microscope equipped with a 40× (0.75 NA) objective and analyzed using ImageJ software as previously described for TMR–dextran uptake (Erami et al., 2017). The scale was set to 3100 pixels/mm and background subtraction was performed using a rolling ball radius of 10 pixels. Image adjustment was made using the Image:Adjust:Threshold commands, selecting Dark Background and a threshold value where the macropinosomes were selectively labeled. The resulting thresholded image was compared to a duplicate image to ensure that all puncta were selected; when necessary, manual adjustments were made to the threshold value. The same threshold value was applied to all subsequent images in the same data set. Using the phase-contrast image, the outline of each cell was traced and superimposed on the thresholded image. The total threshold area was calculated, divided by the number of cells in each field and expressed as average fluorescence area/cell.

Macropinocytosis assay

NIH3T3 cells were seeded as described above and starved overnight in DMEM supplemented with 0.2% BSA and 0.5% FBS. PDGF-BB (0.5 nM) and 70 kDa TMR–dextran (1 mg/ml) were added to the cells for 30 min at 37°C. MDA-MB-231 cells were seeded on glass and cultured overnight in DMEM supplemented with 0.2% BSA, and then incubated with HGF (50 ng/ml) and 70 kDa TMR–dextran (1 mg/ml) for 30 min at 37°C. BT-549 and PC3 cells were plated on glass and grown in complete medium overnight. Cells were incubated with 70 kDa TMR-dextran (1 mg/ml) for 30 min at 37°C. In all cases, dishes were transferred to ice, washed five times with ice-cold PBS, fixed using 4% paraformaldehyde for 20 min at room temperature, washed three times with PBS and mounted. Image acquisition was performed as described above, using a 40× (0.75 NA) objective; for PC3 cells, 0.77 µm sections were taken with a 63×1.4 N.A. objective on a Leica SP5 AOBS confocal microscope. Images were analyzed using ImageJ software as described above, except that macropinosomes were defined as particles greater than 0.75 µm in diameter using the Analyze Particle function.

Circular dorsal ruffle assay

NIH3T3 cells were seeded as described above. Cells were cultured overnight in DMEM supplemented with 0.2% BSA, 0.5% FBS. PDGF-BB (0.5 nM) was added for the specified times at 37°C. Cells were fixed using 4% paraformaldehyde, permeabilized for 3 min with 0.05% Triton X-100, 4% paraformaldehyde and blocked with PBS containing 1% BSA for 1 h at room temperature. Samples were then stained for actin and cortactin, washed three times for 10 min and mounted for microscopy. Samples were imaged using a 40× (0.75 NA) objective. For each experiment, ten random fields were selected and circular dorsal ruffles (CDRs) were identified as actin- and cortactin-positive circular structures at the dorsal surface of the cells. The number of cells showing CDRs was counted, as were the number of CDRs per cell. CDR area was determined on superimposed actin and cortactin images using the polygon selection function to measure the circumference of dorsal circular ruffles positive for both proteins. The CDR area was averaged for each condition and plotted. 868, 380 and 493 cells were examined for lentivirus control, p110β KO and p110α KO, respectively; 710, 624 and 646 cells were counted for DMSO, BYL719 and TGX-211 treatments, respectively.

Live-cell imaging

NIH3T3 cells were seeded and cultured as described above. HEPES (10 mM) was added to the medium, and cells were placed on a heated stage. Images were recorded at 10-s intervals for a total of 30 min, using a 20× (0.5 NA) objective. PDGF-BB (0.5 nM) was added 1 min after the beginning of imaging. Time-lapse images were then stacked using ImageJ software.

Western blotting

Cells were pretreated with inhibitors and/or growth factors as indicated, then lysed with ice-cold lysis buffer [150 mM sodium chloride, 50 mM Tris-HCl pH 7.4, 1 mM orthovanadate, 1% Triton X-100, 5 mM sodium pyrophosphate, 0.25% deoxycholate, 5 mM EDTA, 100 mM sodium fluoride, 100 µM PMSF, and the Pierce™ Protease Inhibitor Mini Tablets (A32955)]. Lysates were clarified by centrifugation at 13,000 *g* for 10 min at 4°C, and protein concentrations were determined using the DC™ (Detergent Compatible) protein assay kit (Bio-Rad). Lysates containing 100 µg of protein were mixed with sample buffer and DTT (100 mM), boiled for 5 min and analyzed by western blotting with SuperSignal™ West Pico PLUS Chemiluminescent Substrate (Thermo Scientific). Gels were quantitated by densitometry using Image Studio Lite (LI-COR Biosciences).

Statistical analysis

Data are expressed as the mean±s.e.m. from three independent experiments unless otherwise indicated. Statistical analyses were conducted using one-way ANOVA.

Author contributions
Conceptualization: G.S., A.R.B., J.M.B.; Methodology: G.S., C.T.J., Z.E., A.R.B., J.M.B.; Formal analysis: G.S.; Investigation: G.S., J.M.B.; Resources: G.S., C.T.J., Z.E., S.D.H.; Writing - original draft: G.S.; Writing - review & editing: A.R.B., J.M.B.; Supervision: A.R.B., J.M.B.; Project administration: A.R.B., J.M.B.; Funding acquisition: A.R.B., J.M.B.

References
Amyere, M., Payrastre, B., Krause, U., Van Der Smissen, P., Veithen, A. and Courtoy, P. J. (2000). Constitutive macropinocytosis in oncogene-transformed fibroblasts depends on sequential permanent activation of phosphoinositide 3-kinase and phospholipase C. *Mol. Biol. Cell* **11**, 3453-3467. doi:10.1091/mbc.11.10.3453

Araki, N., Johnson, M. T. and Swanson, J. A. (1996). A role for phosphoinositide 3-kinase in the completion of macropinocytosis and phagocytosis by macrophages. *J. Cell Biol.* **135**, 1249-1260. doi:10.1083/jcb.135.5.1249

Araki, N., Egami, Y., Watanabe, Y. and Hatae, T. (2007). Phosphoinositide metabolism during membrane ruffling and macropinosome formation in EGF-stimulated A431 cells. *Exp. Cell Res.* **313**, 1496-1507. doi:10.1016/j.yexcr.2007.02.012

Ard, R., Mulatz, K., Pomoransky, J. L., Parks, R. J., Trinkle-Mulcahy, L., Bell, J. C. and Gee, S. H. (2015). Regulation of macropinocytosis by diacylglycerol kinase zeta. *PLoS ONE* **10**, e0144942. doi:10.1371/journal.pone.0144942

Aznar, N., Midde, K. K., Dunkel, Y., Lopez-Sanchez, I., Pavlova, Y., Marivin, A., Barbazán, J., Murray, F., Nitsche, U., Janssen, K.-P. et al. (2015). Daple is a novel non-receptor GEF required for trimeric G protein activation in Wnt signaling. *eLife* **4**, e07091. doi:10.7554/eLife.07091

Bar-Sagi, D. and Feramisco, J. R. (1986). Induction of membrane ruffling and fluid-phase pinocytosis in quiescent fibroblasts by ras proteins. *Science* **233**, 1061-1068. doi:10.1126/science.3090687

Bloomfield, G. and Kay, R. R. (2016). Uses and abuses of macropinocytosis. *J. Cell Sci.* **129**, 2697-2705. doi:10.1242/jcs.176149

Bohdanowicz, M. and Grinstein, S. (2013). Role of phospholipids in endocytosis, phagocytosis, and macropinocytosis. *Physiol. Rev.* **93**, 69-106. doi:10.1152/physrev.00002.2012

Bokoch, G. M., Vlahos, C. J., Wang, Y., Knaus, U. G. and Traynor-Kaplan, A. E. (1996). Rac GTPase interacts specifically with phosphatidylinositol 3-kinase. *Biochem. J.* **315**, 775-779. doi:10.1042/bj3150775

Canton, J. (2018). Macropinocytosis: new insights into its underappreciated role in innate immune cell surveillance. *Front. Immunol.* **9**, 2286. doi:10.3389/fimmu.2018.02286

Canton, J., Schlam, D., Breuer, C., Gütschow, M., Glogauer, M. and Grinstein, S. (2016). Calcium-sensing receptors signal constitutive macropinocytosis and facilitate the uptake of NOD2 ligands in macrophages. *Nat. Commun.* **7**, 11284. doi:10.1038/ncomms11284

Ciraolo, E., Iezzi, M., Marone, R., Marengo, S., Curcio, C., Costa, C., Azzolino, O., Gonella, C., Rubinetto, C., Wu, H. et al. (2008). Phosphoinositide 3-kinase p110beta activity: key role in metabolism and mammary gland cancer but not development. *Sci. Signal.* **1**, ra3. doi:10.1126/scisignal.1161577

Commisso, C., Davidson, S. M., Soydaner-Azeloglu, R. G., Parker, S. J., Kamphorst, J. J., Hackett, S., Grabocka, E., Nofal, M., Drebin, J. A., Thompson, C. B. et al. (2013). Macropinocytosis of protein is an amino acid supply route in Ras-transformed cells. *Nature* **497**, 633-637. doi:10.1038/nature12138

Dbouk, H. A., Vadas, O., Shymanets, A., Burke, J. E., Salamon, R. S., Khalil, B. D., Barrett, M. O., Waldo, G. L., Surve, C., Hsueh, C. et al. (2012). G protein-coupled receptor-mediated activation of p110beta by Gbetagamma is required for cellular transformation and invasiveness. *Sci. Signal.* **5**, ra89. doi:10.1126/scisignal.2003264

de Carvalho, T. M. U., Barrias, E. S. and de Souza, W. (2015). Macropinocytosis: a pathway to protozoan infection. *Front. Physiol.* **6**, 106. doi:10.3389/fphys.2015.00106

Delcourt, N., Bockaert, J. and Marin, P. (2007). GPCR-jacking: from a new route in RTK signalling to a new concept in GPCR activation. *Trends Pharmacol. Sci.* **28**, 602-607. doi:10.1016/j.tips.2007.09.007

Dharmawardhane, S., Schürmann, A., Sells, M. A., Chernoff, J., Schmid, S. L. and Bokoch, G. M. (2000). Regulation of macropinocytosis by p21-activated kinase-1. *Mol. Biol. Cell* **11**, 3341-3352. doi:10.1091/mbc.11.10.3341

Erami, Z., Khalil, B. D., Salloum, G., Yao, Y., LoPiccolo, J., Shymanets, A., Nürnberg, B., Bresnick, A. R. and Backer, J. M. (2017). Rac1-stimulated macropinocytosis enhances Gbetagamma activation of PI3Kbeta. *Biochem. J.* **474**, 3903-3914. doi:10.1042/BCJ20170279

Erami, Z., Heitz, S., Bresnick, A. R. and Backer, J. M. (2019). PI3Kbeta links integrin activation and PI(3,4)P2 production during invadopodial maturation. *Mol. Biol. Cell* (in press). doi:10.1091/mbc.E19-03-0182

Fritsch, R., de Krijger, I., Fritsch, K., George, R., Reason, B., Kumar, M. S., Diefenbacher, M., Stamp, G. and Downward, J. (2013). RAS and RHO families of GTPases directly regulate distinct phosphoinositide 3-kinase isoforms. *Cell* **153**, 1050-1063. doi:10.1016/j.cell.2013.04.031

Garcia-Marcos, M., Ghosh, P. and Farquhar, M. G. (2009). GIV is a nonreceptor GEF for G alpha i with a unique motif that regulates Akt signaling. *Proc. Natl. Acad. Sci. USA* **106**, 3178-3183. doi:10.1073/pnas.0900294106

Goulden, B. D., Pacheco, J., Dull, A., Zewe, J. P., Deiters, A. and Hammond, G. R. V. (2018). A high-avidity biosensor reveals plasma membrane PI(3,4)P2 is predominantly a class I PI3K signaling product. *J. Cell Biol.* **218**, 1066-1079. doi:10.1083/jcb.201809026

Guillermet-Guibert, J., Bjorklof, K., Salpekar, A., Gonella, C., Ramadani, F., Bilancio, A., Meek, S., Smith, A. J. H., Okkenhaug, K. and Vanhaesebroeck, B. (2008). The p110beta isoform of phosphoinositide 3-kinase signals downstream of G protein-coupled receptors and is functionally redundant with p110gamma. *Proc. Natl. Acad. Sci. USA* **105**, 8292-8297. doi:10.1073/pnas.0707761105

Hasegawa, J., Tokuda, E., Tenno, T., Tsujita, K., Sawai, H., Hiroaki, H., Takenawa, T. and Itoh, T. (2011). SH3YL1 regulates dorsal ruffle formation by a novel phosphoinositide-binding domain. *J. Cell Biol.* **193**, 901-916. doi:10.1083/jcb.201012161

Hawkins, P. T. and Stephens, L. R. (2016). Emerging evidence of signalling roles for PI(3,4)P2 in Class I and II PI3K-regulated pathways. *Biochem. Soc. Trans.* **44**, 307-314. doi:10.1042/BST20150248

Hawkins, P. T., Eguinoa, A., Qiu, R.-G., Stokoe, D., Cooke, F. T., Walters, R., Wennström, S., Claesson-Welsh, L., Evans, T., Symons, M. et al. (1995). PDGF stimulates an increase in GTP-Rac via activation of phosphoinositide 3-kinase. *Curr. Biol.* **5**, 393-403. doi:10.1016/S0960-9822(95)00080-7

Heitz, S. D., Hamelin, D. J., Hoffmann, R. M., Greenberg, N., Salloum, G., Erami, Z., Khalil, B. D., Shymanets, A., Steidle, E. A., Gong, G. Q. et al. (2019). A single discrete rab5-binding site in PI3Kbeta is required for tumor cell invasion. *J. Biol. Chem.* **294**, 4621-4633. doi:10.1074/jbc.RA118.006032

Hiles, I. D., Otsu, M., Volinia, S., Fry, M. J., Gout, I., Dhand, R., Panayotou, G., Ruiz-Larrea, F., Thompson, A., Totty, N. F. et al. (1992). Phosphatidylinositol 3-kinase: structure and expression of the 110 kd catalytic subunit. *Cell* **70**, 419-429. doi:10.1016/0092-8674(92)90166-A

Hodakoski, C., Hopkins, B. D., Zhang, G., Su, T., Cheng, Z., Morris, R., Rhee, K. Y., Goncalves, M. D. and Cantley, L. C. (2019). Rac-mediated macropinocytosis of extracellular protein promotes glucose independence in non-small cell lung cancer. *Cancers (Basel)* **11**, 37. doi:10.3390/cancers11010037

Hoeller, O., Bolourani, P., Clark, J., Stephens, L. R., Hawkins, P. T., Weiner, O. D., Weeks, G. and Kay, R. R. (2013). Two distinct functions for PI3-kinases in macropinocytosis. *J. Cell Sci.* **126**, 4296-4307. doi:10.1242/jcs.134015

Houslay, D. M., Anderson, K. E., Chessa, T., Kulkarni, S., Fritsch, R., Downward, J., Backer, J. M., Stephens, L. R. and Hawkins, P. T. (2016). Coincident signals from GPCRs and receptor tyrosine kinases are uniquely transduced by PI3Kbeta in myeloid cells. *Sci. Signal.* **9**, ra82. doi:10.1126/scisignal.aae0453

Hu, P., Mondino, A., Skolnik, E. Y. and Schlessinger, J. (1993). Cloning of a novel, ubiquitously expressed human phosphatidylinositol 3-kinase and identification of its binding site on p85. *Mol. Cell. Biol.* **13**, 7677-7688. doi:10.1128/MCB.13.12.7677

Jia, S., Liu, Z., Zhang, S., Liu, P., Zhang, L., Lee, S. H., Zhang, J., Signoretti, S., Loda, M., Roberts, T. M. et al. (2008). Essential roles of PI(3)K-p110beta in cell growth, metabolism and tumorigenesis. *Nature* **454**, 776-779. doi:10.1038/nature07091

Khalil, B. D., Hsueh, C., Cao, Y., Abi Saab, W. F., Wang, Y., Condeelis, J. S., Bresnick, A. R. and Backer, J. M. (2016). GPCR signaling mediates tumor metastasis via PI3Kbeta. *Cancer Res.* **76**, 2944-2953. doi:10.1158/0008-5472.CAN-15-1675

Kim, S. M., Nguyen, T. T., Ravi, A., Kubiniok, P., Finicle, B. T., Jayashankar, V., Malacrida, L., Hou, J., Robertson, J., Gao, D. et al. (2018). PTEN deficiency and AMPK activation promote nutrient scavenging and anabolism in prostate cancer cells. *Cancer Discov.* **8**, 866-883. doi:10.1158/2159-8290.CD-17-1215

Koivusalo, M., Welch, C., Hayashi, H., Scott, C. C., Kim, M., Alexander, T., Touret, N., Hahn, K. M. and Grinstein, S. (2010). Amiloride inhibits macropinocytosis by lowering submembranous pH and preventing Rac1 and Cdc42 signaling. *J. Cell Biol.* **188**, 547-563. doi:10.1083/jcb.200908086

Lee, B. C., Lee, T. H., Avraham, S. and Avraham, H. K. (2004). Involvement of the chemokine receptor CXCR4 and its ligand stromal cell-derived factor 1alpha in breast cancer cell migration through human brain microvascular endothelial cells. *Mol. Cancer Res.* **2**, 327-338.

Leverrier, Y., Okkenhaug, K., Sawyer, C., Bilancio, A., Vanhaesebroeck, B. and Ridley, A. J. (2003). Class I phosphoinositide 3-kinase p110beta is required for apoptotic cell and Fcgamma receptor-mediated phagocytosis by macrophages. *J. Biol. Chem.* **278**, 38437-38442. doi:10.1074/jbc.M306649200

Leyme, A., Marivin, A., Perez-Gutierrez, L., Nguyen, L. T. and Garcia-Marcos, M. (2015). Integrins activate trimeric G proteins via the nonreceptor protein GIV/Girdin. *J. Cell Biol.* **210**, 1165-1184. doi:10.1083/jcb.201506041

Lim, J. P. and Gleeson, P. A. (2011). Macropinocytosis: an endocytic pathway for internalising large gulps. *Immunol. Cell Biol.* **89**, 836-843. doi:10.1038/icb.2011.20

Maekawa, M., Terasaka, S., Mochizuki, Y., Kawai, K., Ikeda, Y., Araki, N., Skolnik, E. Y., Taguchi, T. and Arai, H. (2014). Sequential breakdown of 3-phosphorylated phosphoinositides is essential for the completion of macropinocytosis. *Proc. Natl. Acad. Sci. USA* **111**, E978-E987. doi:10.1073/pnas.1311029111

Mellström, K., Heldin, C.-H. and Westermark, B. (1988). Induction of circular membrane ruffling on human fibroblasts by platelet-derived growth factor. *Exp. Cell Res.* **177**, 347-359. doi:10.1016/0014-4827(88)90468-5

Ni, J., Liu, Q., Xie, S., Carlson, C., Von, T., Vogel, K., Riddle, S., Benes, C., Eck, M., Roberts, T. et al. (2012). Functional characterization of an isoform-selective inhibitor of PI3K-p110beta as a potential anticancer agent. *Cancer Discov.* **2**, 425-433. doi:10.1158/2159-8290.CD-12-0003

Nishiyama, T., Sasaki, T., Takaishi, K., Kato, M., Yaku, H., Araki, K., Matsuura, Y. and Takai, Y. (1994). Rac P21 is involved in insulin-induced membrane ruffling and rho P21 is involved in hepatocyte growth factor- and 12-O-

Tetradecanoylphorbol-13-Acetate (Tpa)-induced membrane ruffling in Kb cells. *Mol. Cell. Biol.* **14**, 2447-2456. doi:10.1128/MCB.14.4.2447

Pacitto, R., Gaeta, I., Swanson, J. A. and Yoshida, S. (2017). CXCL12-induced macropinocytosis modulates two distinct pathways to activate mTORC1 in macrophages. *J. Leukoc. Biol.* **101**, 683-692. doi:10.1189/jlb.2A0316-141RR

Palm, W., Araki, J., King, B., DeMatteo, R. G. and Thompson, C. B. (2017). Critical role for PI3-kinase in regulating the use of proteins as an amino acid source. *Proc. Natl. Acad. Sci. USA* **114**, E8628-E8636. doi:10.1073/pnas. 1712726114

Racoosin, E. L. and Swanson, J. A. (1992). M-CSF-induced macropinocytosis increases solute endocytosis but not receptor-mediated endocytosis in mouse macrophages. *J. Cell Sci.* **102**, 867-880.

Redelman-Sidi, G., Binyamin, A., Gaeta, I., Palm, W., Thompson, C. B., Romesser, P. B., Lowe, S. W., Bagul, M., Doench, J. G., Root, D. E. et al. (2018). The Canonical Wnt Pathway Drives Macropinocytosis in Cancer. *Cancer Res.* **78**, 4658-4670. doi:10.1158/0008-5472.CAN-17-3199

Redka, D. S., Gütschow, M., Grinstein, S. and Canton, J. (2018). Differential ability of proinflammatory and anti-inflammatory macrophages to perform macropinocytosis. *Mol. Biol. Cell* **29**, 53-65. doi:10.1091/mbc.E17-06-0419

Ridley, A. J., Comoglio, P. M. and Hall, A. (1995). Regulation of scatter factor/ hepatocyte growth factor responses by Ras, Rac, and Rho in MDCK cells. *Mol. Cell. Biol.* **15**, 1110-1122. doi:10.1128/MCB.15.2.1110

Roach, T. I. A., Rebres, R. A., Fraser, I. D. C., Decamp, D. L., Lin, K.-M., Sternweis, P. C., Simon, M. I. and Seaman, W. E. (2008). Signaling and cross-talk by C5a and UDP in macrophages selectively use PLCbeta3 to regulate intracellular free calcium. *J. Biol. Chem.* **283**, 17351-17361. doi:10.1074/jbc. M800907200

Rodriguez-Viciana, P., Warne, P. H., Khwaja, A., Marte, B. M., Pappin, D., Das, P., Waterfield, M. D., Ridley, A. and Downward, J. (1997). Role of phosphoinositide 3-OH kinase in cell transformation and control of the actin cytoskeleton by Ras. *Cell* **89**, 457-467. doi:10.1016/S0092-8674(00)80226-3

Sobhy, H. (2017). A comparative review of viral entry and attachment during large and giant dsDNA virus infections. *Arch. Virol.* **162**, 3567-3585. doi:10.1007/ s00705-017-3497-8

Swanson, J. A. (1989). Phorbol esters stimulate macropinocytosis and solute flow through macrophages. *J. Cell Sci.* **94**, 135-142.

Swanson, J. A. (2008). Shaping cups into phagosomes and macropinosomes. *Nat. Rev. Mol. Cell Biol.* **9**, 639-649. doi:10.1038/nrm2447

Tolias, K. F., Cantley, L. C. and Carpenter, C. L. (1995). Rho family GTPases bind to phosphoinositide kinases. *J. Biol. Chem.* **270**, 17656-17659. doi:10.1074/jbc. 270.30.17656

Veltman, D. M., Williams, T. D., Bloomfield, G., Chen, B.-C., Betzig, E., Insall, R. H. and Kay, R. R. (2016). A plasma membrane template for macropinocytic cups. *eLife* **5**, e20085. doi:10.7554/eLife.20085

Wee, S., Wiederschain, D., Maira, S.-M., Loo, A., Miller, C., deBeaumont, R., Stegmeier, F., Yao, Y.-M. and Lengauer, C. (2008). PTEN-deficient cancers depend on *PIK3CB*. *Proc. Natl. Acad. Sci. USA* **105**, 13057-13062. doi:10.1073/ pnas.0802655105

Welliver, T. P. and Swanson, J. A. (2012). A growth factor signaling cascade confined to circular ruffles in macrophages. *Biol Open* **1**, 754-760. doi:10.1242/ bio.20121784

Wennström, S., Hawkins, P., Cooke, F., Hara, K., Yonezawa, K., Kasuga, M., Jackson, T., Claesson-Welsh, L. and Stephens, L. (1994). Activation of phosphoinositide 3-kinase is required for PDGF-stimulated membrane ruffling. *Curr. Biol.* **4**, 385-393. doi:10.1016/S0960-9822(00)00087-7

West, M. A., Prescott, A. R., Eskelinen, E.-L., Ridley, A. J. and Watts, C. (2000). Rac is required for constitutive macropinocytosis by dendritic cells but does not control its downregulation. *Curr. Biol.* **10**, 839-848. doi:10.1016/S0960-9822(00)00595-9

Yoshida, S., Hoppe, A. D., Araki, N. and Swanson, J. A. (2009). Sequential signaling in plasma-membrane domains during macropinosome formation in macrophages. *J. Cell Sci.* **122**, 3250-3261. doi:10.1242/jcs.053207

Yoshida, S., Pacitto, R., Yao, Y., Inoki, K. and Swanson, J. A. (2015). Growth factor signaling to mTORC1 by amino acid-laden macropinosomes. *J. Cell Biol.* **211**, 159-172. doi:10.1083/jcb.201504097

Yoshida, S., Pacitto, R., Sesi, C., Kotula, L. and Swanson, J. A. (2018). Dorsal ruffles enhance activation of Akt by growth factors. *J. Cell Sci.* **131**, jcs220517. doi:10.1242/jcs.220517

Yuzugullu, H., Baitsch, L., Von, T., Steiner, A., Tong, H., Ni, J., Clayton, L. K., Bronson, R., Roberts, T. M., Gritsman, K. et al. (2015). A PI3K p110beta-Rac signalling loop mediates Pten-loss-induced perturbation of haematopoiesis and leukaemogenesis. *Nat. Commun.* **6**, 8501. doi:10.1038/ncomms9501

Zheng, Y., Bagrodia, S. and Cerione, R. A. (1994). Activation of phosphoinositide 3-kinase activity by Cdc42Hs binding to p85. *J. Biol. Chem.* **269**, 18727-18730.